arXiv:1211.0772v1 [cond-mat.mes-hall] 5 Nov 2012

Topological Invariants of Metals and Related Physical Effects

Jianhui Zhou,[1] Hua Jiang,[2] Qian Niu,[2, 3] and Junren Shi[2]

[1] *Beijing National Laboratory for Condensed Matter Physics and Institute of Physics, Chinese Academy of Sciences, Beijing 100190, China*
[2] *International Center for Quantum Materials, Peking University , Beijing 100871, China*
[3] *Department of Physics, The University of Texas, Austin, Texas 78712-0264, USA*

The total reciprocal space magnetic flux threading through a closed Fermi surface is a topological invariant for a three-dimensional metal. For a Weyl metal, the invariant is non-zero for each of its Fermi surfaces. We show that such an invariant can be related to magneto-valley-transport effect, in which an external magnetic field can induce a valley current. We further show that a strain field can drive an electric current, and the effect is dictated by a second class Chern invariant. These connections open the pathway to observe the hidden topological invariants in metallic systems.

PACS numbers: 71.10.Ay, 75.47.-m, 72.10.Bg

There have been great successes in classifying insulators using topological invariants, such as the TKNN number for quantum Hall insulators[1], and the Z_2 index for insulators with time-reversal symmetry [2]. The classification can even be extended to the more general systems such as superconductors [3]. In all of these systems, there exist gaps in their excitation spectrums, which provide topological protection, and resulting in robust physical effects.

For metallic systems, there are also topological invariants. An apparent one is the total volume enclosed by Fermi surface in a non-magnetic metal, according to Luttinger's theorem. One may find other topological invariants, and in some cases, even relate them to observable physical effects [4, 5]. For instance, in a two dimensional (2D) metallic system with time reversal symmetry, an electron moving around the Fermi cycle in the reciprocal space will acquire a total Berry phase of either 0 or π per cycle. The non-trivial π Berry phase is responsible for the unusual anti-weak localization effect observed in compounds such as graphene or the surface states of three-dimensional (3D) topological insulators [6]. It can even modify the effective electron-electron interaction, giving rise to unconventional superconducting pairing symmetries [7–9].

For a 3D metal, an apparent topological invariant is the total reciprocal space magnetic flux threading through a closed Fermi surface:

$$\Phi_{FS} \equiv \int_{FS} \boldsymbol{\Omega} \cdot \mathrm{d}\boldsymbol{S}_F \,, \tag{1}$$

where $\boldsymbol{\Omega}(\boldsymbol{k})$ is the Berry curvature of the Bloch electron in band forming the Fermi surface at quasi-momentum $\boldsymbol{k}$, defined by $\boldsymbol{\Omega}(\boldsymbol{k}) = i \langle \nabla_{\boldsymbol{k}} u(\boldsymbol{k})| \times |\nabla_{\boldsymbol{k}} u(\boldsymbol{k})\rangle$, and $|u(\boldsymbol{k})\rangle$ is the corresponding periodic part of Bloch wave function [10, 11]. Φ_{FS} is quantized as

$$\Phi_{FS} = 2\pi n \,, \tag{2}$$

with n being an integer. A nonzero quantized number n indicates the topological nature of the metal. The topological number n cannot be changed without changing the geometric topology of the Fermi surface. It is easy to generalize the classification to the more general metallic systems with multiple Fermi surfaces. In this case, one can assign a topological number to each of the Fermi surfaces, and the numbers cannot be changed without merging/splitting of the Fermi surfaces. An example of such topologically non-trivial 3D metals is the 3D Weyl (semi-)metal, in which the Fermi surfaces enclose Weyl nodes that give rise to the quantized reciprocal magnetic fluxes [12–17]. An immediate question is how the topological invariant can be related to observable physical effects.

In this Letter, we will show that the invariant can be related to the magneto-valley-transport property of the 3D topological metals. We show that a magnetic field will induce an electric current along the direction of the magnetic field in each of the Fermi pockets. For a 3D metal that always has an even number of Dirac points (due to the Fermion doubling theorem), such a response will generate a valley-current response, with the valleys corresponding to the Dirac fermions of opposite helicities. On the other hand, using carefully engineered strain field, one could create an effective magnetic field that has the opposite directions in the two different valleys, generating a real electric current response. We will show that such response is related to a second-class Chern number defined on the Fermi surfaces and the real space.

To see the response of the system to an applied magnetic field, we use the semiclassical wave packet dynamics [10, 11]. The equations of motion for the wave-packet center position $\boldsymbol{r}$ and momentum $\boldsymbol{k}$ in the presence of a magnetic field $\boldsymbol{B}$ can be written as,

$$\dot{\boldsymbol{r}} = \boldsymbol{v}_n(\boldsymbol{k}) - \dot{\boldsymbol{k}} \times \boldsymbol{\Omega}_n(\boldsymbol{k}) \tag{3}$$

$$\hbar\dot{\boldsymbol{k}} = -e\dot{\boldsymbol{r}} \times \boldsymbol{B} \tag{4}$$

where $\Omega_n(\boldsymbol{k})$ is the Berry curvature of Bloch states of the n-th band, and $v_n(\boldsymbol{k}) = \partial\tilde{\epsilon}_n(\boldsymbol{k})/\partial\hbar\boldsymbol{k}$ is the group velocity of Bloch electrons and $\tilde{\epsilon}_n(\boldsymbol{k})$ is the band dispersion. We note that although the set of equations is semi-classical, it is versatile in deriving results valid in

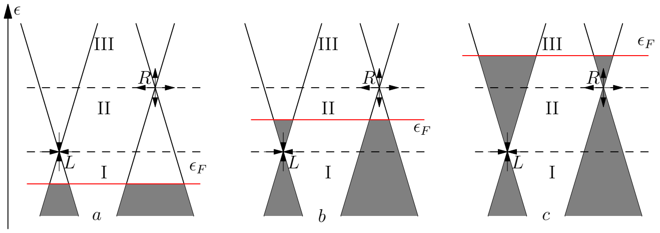

Figure 1: A schematic plot to show that the electric current response to a magnetic field for a real 3D metal is always zero because the contribution from the two Dirac points always cancel each other. Note that for each individual Dirac point, the contributions from the lower and the upper bands have the same sign, because the normal directions (directions of the group velocities) of the iso-energy surfaces are opposite.

quantum regime. Actually one can establish that the result derived from the semiclassical equations are in general valid as long as the external fields are weak in the length scales of the lattice constants.

It is straightforward to get:

$$D_n\left(\boldsymbol{k}\right)\dot{\boldsymbol{r}}=\boldsymbol{v}_n\left(\boldsymbol{k}\right)+\frac{e}{\hbar}\left(v_n\cdot\boldsymbol{\Omega}_n\right)\boldsymbol{B} \tag{5}$$

where $D_n\left(\boldsymbol{k}\right)\equiv 1+\left(e/\hbar\right)\left(\boldsymbol{B}\cdot\boldsymbol{\Omega}_n\right)$ stands for the Berry curvature's correction to the density of states in phase space [18]. We obtain a response of the electric current $\boldsymbol{j}_B$ in the direction parallel to the applied magnetic field $\boldsymbol{B}$:

$$\boldsymbol{j}_B=-e\sum_n\int D_n\left(\boldsymbol{k}\right)\dot{\boldsymbol{r}}f\left(\tilde{\epsilon}_n\left(\boldsymbol{k}\right)\right)\left[d\boldsymbol{k}\right]=\alpha_B\boldsymbol{B} \tag{6}$$

where the magneto-current response coefficient is defined by

$$\begin{aligned}\alpha_B &\equiv -\frac{e^2}{\hbar}\sum_n\int\left(\boldsymbol{v}_n\cdot\boldsymbol{\Omega}_n\right)f\left(\tilde{\epsilon}_n\left(\boldsymbol{k}\right)\right)\left[d\boldsymbol{k}\right] &(7)\\ &= -\frac{e^2}{h^2}\sum_n\int\Phi_\epsilon^{(n)}f\left(\epsilon\right)\frac{d\epsilon}{2\pi} &(8)\end{aligned}$$

where $\Phi_\epsilon^{(n)}\equiv\int_{\tilde{\epsilon}_n(\boldsymbol{k})=\epsilon}d\vec{S}\cdot\boldsymbol{\Omega}_n$ stands for the flux threading through the iso-energy surface at ϵ for n-th band, with the normal direction of the $d\vec{S}$ being defined as the direction of the group velocity $\boldsymbol{v}_n(\boldsymbol{k})$, and $f\left(\epsilon\right)$ is the Fermi distribution function, $[d\boldsymbol{k}]\equiv\mathrm{d}\boldsymbol{k}/(2\pi)^3$.

However, for a real 3D metal, the total electric current response is always zero. This is because the Dirac points, which are the source of the reciprocal space magnetic field fluxes, always appear in pairs in the reciprocal space, and in the opposite helicities, according to the fermion doubling theorem [19]. As shown in Fig. 1, the reciprocal space magnetic fluxes from such a pair of Dirac points always cancel each other at all the energies. As a result, the magneto-current response coefficient α_B is always zero for a real 3D metal.

On the other hand, one can construct a non-zero response of valley current for systems with nontrivial topological numbers of Fermi surfaces. To be specific, we consider a 3D Weyl (semi-)metal [12–17]. The simplest form of such a metal comprises of a pair of Weyl nodes that have the reciprocal magnetic monopole charge $\pm 2\pi n$. When the two Weyl nodes are well separated in the momentum space and the Fermi level is close to the energy of the Weyl nodes, the electrons in the two Fermi pockets centering around the Weyl nodes can be considered as two independent fermion species, and we can introduce a new "valley" degree of freedom to label them. An external magnetic field will induced the opposite electric currents in the two valleys at the zero temperature:

$$\boldsymbol{j}_\pm=\pm n\frac{e^2}{h^2}\left(\epsilon_F-\epsilon_0\right)\boldsymbol{B}\,, \tag{9}$$

where ± denotes the valley index, ϵ_F is the Fermi energy and ϵ_0 is the energy of the Weyl nodes. The corresponding valley current is:

$$\begin{aligned}\boldsymbol{j}_v &= \boldsymbol{j}_+-\boldsymbol{j}_-\,, &(10)\\ &= n\frac{2e^2}{h^2}\left(\epsilon_F-\epsilon_0\right)\boldsymbol{B}\,. &(11)\end{aligned}$$

Although the introduction of the valley degree of freedom is based upon the separation of momentum space, and looks artificial, it can actually be as real as the other degrees of freedom such as spin, within the certain energy and momentum scales. In particular, when $n=1$, a pair of Weyl nodes can be mapped to the right-handed and left-handed neutrinos respectively, albeit in a much lower energy scale. When the system is clean enough or only has the spatially smooth disorders, the scattering between the two valleys is negligible, and the electron can maintain its valley identity for a sufficient long time. In this case, one expects a valley accumulation in the boundary of the system when there is a bulk valley current, as shown in Fig. 2. The detailed profile of such an accumulation depends on the condition of the sample boundary and the valley relaxation.

Earlier attempts to utilize the valley degree of freedom are mainly focused on the graphene-based systems [20–23]. More recently, the monolayer molybdenum disulphide (MoS_2) is proposed to be an ideal material for valleytronics [24, 25]. Our analysis shows that the Weyl metals can also be a candidate for the valleytronics, and the valley polarization can be achieved by applying a magnetic field.

Next, we consider the possibility for generating a real electric current in a 3D metal by applying a strain field. A carefully engineered strain field could induce artificial magnetic field with its magnitude and direction depending on the momentum [26, 27]. Such an artificial magnetic field can have the opposite directions in the different valleys, as observed in graphene [28]. If this can be done

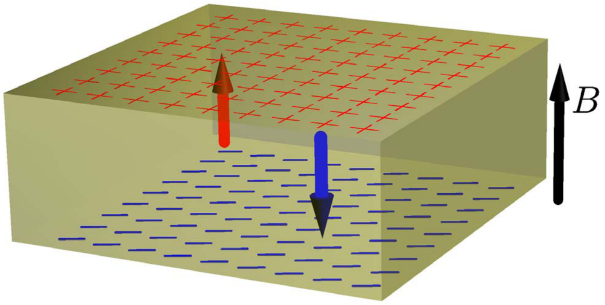

Figure 2: The magnetic field induced valley polarization. The magnetic field $\boldsymbol{B}$ (black arrow) will induce counter-propagating currents of Weyl electrons of the opposite helicities (red and blue arrows). It results in an accumulation of right-handed (+) and left-handed (-) Weyl electrons at the two ends of samples, respectively.

in a Weyl metal, from Eq. (9), it will generate a real electric current.

The proper framework to consider the effect is to use the complete form of semiclassical equation:

$$\dot{\boldsymbol{r}} = \boldsymbol{v}(\boldsymbol{k},\boldsymbol{r}) - \overleftrightarrow{\Omega}^{\boldsymbol{kr}}\cdot\dot{\boldsymbol{r}} - \overleftrightarrow{\Omega}^{\boldsymbol{kk}}\cdot\dot{\boldsymbol{k}}, \tag{12}$$

$$\dot{\boldsymbol{k}} = \overleftrightarrow{\Omega}^{\boldsymbol{rk}}\cdot\dot{\boldsymbol{k}} + \overleftrightarrow{\Omega}^{\boldsymbol{rr}}\cdot\dot{\boldsymbol{r}}, \tag{13}$$

where $\boldsymbol{v}(\boldsymbol{k},\boldsymbol{r}) = \partial\tilde{\epsilon}(\boldsymbol{k},\boldsymbol{r})/\partial(\hbar\boldsymbol{k})$, $\Omega^{\boldsymbol{kk}}_{\alpha\beta} = -2\mathrm{Im}\,\langle\partial u(\boldsymbol{r},\boldsymbol{k})/\partial k_\alpha\,|\partial u(\boldsymbol{r},\boldsymbol{k})/\partial k_\beta\,\rangle$, $\Omega^{\boldsymbol{kr}}_{\alpha\beta} = -2\mathrm{Im}\,\langle\partial u(\boldsymbol{r},\boldsymbol{k})/\partial k_\alpha\,|\partial u(\boldsymbol{r},\boldsymbol{k})/\partial r_\beta\,\rangle$, and $\overleftrightarrow{\Omega}^{\boldsymbol{rk}}$, $\overleftrightarrow{\Omega}^{\boldsymbol{rr}}$ are defined similarly [10]. Note that in the presence of spatial inhomogeneity due to the strain field, the Bloch wave function and the energy dispersion are in general functions of both the wave packet central momentum $\boldsymbol{k}$ and the central position $\boldsymbol{r}$. As a result, the new components of the Berry curvatures arise. Here, $\overleftrightarrow{\Omega}^{\boldsymbol{rr}}$ assumes the role of that of the magnetic field $\boldsymbol{B}$ in Eq. (4), and can be considered as an artificial magnetic field.

In most of the cases the strain field is weak, and the spatial gradient of the Bloch wave function is a small quantity. One can expand the solution of Eq. (12–13) in the orders of the spatial gradients. To the second order of the spatial gradients, we find that the total electric current density can be written as,

$$\boldsymbol{j}(\boldsymbol{r}) = \boldsymbol{\nabla}_{\boldsymbol{r}}\times\boldsymbol{m}(\boldsymbol{r}) - \frac{e}{\hbar}\int[\mathrm{d}\boldsymbol{k}]f(\tilde{\epsilon})\boldsymbol{\Omega}^{\boldsymbol{kk}}\times\boldsymbol{\nabla}_{\boldsymbol{r}}\tilde{\epsilon} - \frac{e}{2\pi h}\int\boldsymbol{\Phi}^{(2)}_{\epsilon,\boldsymbol{r}}f(\epsilon)\frac{\mathrm{d}\epsilon}{2\pi}, \tag{14}$$

where $\boldsymbol{m}(\boldsymbol{r}) \equiv -(e/\hbar)\int[\mathrm{d}\boldsymbol{k}]\boldsymbol{\Omega}^{\boldsymbol{kk}}g(\tilde{\epsilon})$ with $g(\tilde{\epsilon}) \equiv \int\mathrm{d}\tilde{\epsilon}f(\tilde{\epsilon})$, and we define a vector $\left(\boldsymbol{\Omega}^{\boldsymbol{kk}}\right)_\alpha \equiv (1/2)\epsilon_{\alpha\beta\gamma}\Omega^{\boldsymbol{kk}}_{\beta\gamma}$. $\boldsymbol{\Phi}^{(2)}_{\epsilon,\boldsymbol{r}}$ is the second-class Chern-flux through the momentum space iso-energy surface $S_{\epsilon,\boldsymbol{r}}$ with $\tilde{\epsilon}(\boldsymbol{k},\boldsymbol{r}) = \epsilon$ at the spatial position $\boldsymbol{r}$. Specifically, it is defined as,

$$\Phi^{(2)\alpha}_{\epsilon,\boldsymbol{r}} = \frac{1}{2}\epsilon_{\alpha\beta\gamma}\int_{S_{\epsilon,\boldsymbol{r}}}\mathrm{d}\boldsymbol{k}\left[\Omega^{\boldsymbol{rr}}_{\beta\gamma}\Omega^{\boldsymbol{kk}}_{12} + \Omega^{\boldsymbol{kr}}_{2\beta}\Omega^{\boldsymbol{rk}}_{\gamma1} + \Omega^{\boldsymbol{rk}}_{\beta1}\Omega^{\boldsymbol{kr}}_{2\gamma}\right], \tag{15}$$

where we have defined k_1 and k_2 as the two generalized coordinates for parametrizing the two dimensional iso-energy surface $S_{\epsilon,\boldsymbol{r}}$, with the normal direction of the surface defined by $\boldsymbol{v}$. It is easy to observe that the integrand in Eq. (15) is exactly the second Chern-form of Berry curvature defined in the manifold (r_1, r_2, k_2, k_2), where r_1 and r_2 are the spatial coordinates in the plane perpendicular to the direction of the current.

The electric current density induced by a strain field has three parts of contributions, corresponding to each of the three terms in Eq. (14), respectively: the first term is the magnetization current due to the spatial inhomogeneity; the second term is the anomalous Hall current [29] driven by the electro-elastic potential $-\boldsymbol{\nabla}_{\boldsymbol{r}}\tilde{\epsilon}$; and most importantly, there arises a topological contribution proportional to $\boldsymbol{\Phi}^{(2)}_{\epsilon,\boldsymbol{r}}$. It is easy to see the total current across a cross-section of the sample $I = \int\mathrm{d}\boldsymbol{S}\cdot\boldsymbol{j}$ has a topological contribution dictated by the second Chern number because $\int\mathrm{d}\boldsymbol{S}\cdot\boldsymbol{\Phi}^{(2)}_{\epsilon,\boldsymbol{r}} = (2\pi)^2 n$ with n being an integer, and we have:

$$I_{\mathrm{topo.}} = -\frac{ne}{h}(\epsilon_F - \epsilon_0). \tag{16}$$

We discuss the implications of Eq. (14) and Eq. (16) for different kinds of strain fields. For a strain field created by the usual lattice deformation, one expects that the artificial magnetic field varies spatially, and there cannot be big spatial area with nearly uniform artificial magnetic field, as it costs huge elastic energy to sustain the required strain field [26, 27]. In this case, one cannot expect a net electric current induced by the strain field. This does not exclude the possibility of existence of a local current density which may in turn modify the lattice dynamics.

A particularly interesting case is when the system has topological defect, e.g., a disclination, one expects an artificial magnetic field distributing around the disclination line [26]. A non-zero second Chern number in Eq. (16) implies the existence of a chiral conducting channel along the line of disclination, just like the chiral edge state of a quantum Hall insulator. It is important to note that the chiral conducting channel is in a metal , with its robustness protected by the structure of the topological defect and the Fermi surface topology. The construction of a model system to realize the novel possibility of creating topologically protected chiral modes in a metal is left for future investigations.

In summary, we discuss the topological invariants in three dimensional metals. We find that non-zero reciprocal space magnetic fluxes threading through the Fermi surface will give rise to the magnetic-field-to-valley-current response, although no electric current response is possible due to the Fermion doubling theorem. We further observe that a strain field could induce an electric current dictated by a second Chern number. It implies the possibility of existence of chiral conducting channel in a metallic system with appropriate structural topology and momentum space topology.

This work is supported by 973 program of China (2009CB929101, 2012CB921304). We thank Tao Qin for useful discussion.

---

[1] D. J. Thouless, M. Kohmoto, M. P. Nightingale, and M. den Nijs, Phys. Rev. Lett. **49**, 405 (1982).
[2] C. L. Kane and E. J. Mele, Phys. Rev. Lett. **95**, 146802 (2005).
[3] S. Ryu, A. P. Schnyder, A. Furusaki, and A. W. W. Ludwig, New Journal of Physics **12**, 065010 (2010).
[4] Volovik, G. E. *The Universe in a Helium Droplet*, Clarendon Press, Oxford, 2003.
[5] M. Oshikawa, Phys. Rev. Lett. **84**, 3370 (2000).
[6] H.-Z. Lu, J. Shi, and S.-Q. Shen, Phys. Rev. Lett. **107**, 076801 (2011).
[7] J. Shi and Q. Niu, arXiv:cond-mat:0610531 (2006).
[8] L. Mao, J. Shi, Q. Niu, and C. Zhang, Phys. Rev. Lett. **106**, 157003 (2011).
[9] J. Zhou, T. Qin, J. Shi, arXiv:cond-mat:1205.2936 (2012).
[10] G. Sundaram, and Q. Niu, Phys. Rev. B. **59**, 14915 (1999).
[11] D. Xiao, M. Chang, and Q. Niu, Rev. Mod. Phys. **82**, 1959-2007 (2010).
[12] H. B. Nielsen, and M. Ninomiya, Phys. Lett. B. **130**, 389 (1983).
[13] P. Hosur, P. Ryu, and A. Vishwanath, Phys. Rev. B. **81**, 045120 (2010).
[14] X. Wan, A. M. Turner, A. Vishvanath, and S. Y. Savrasov, Phys. Rev. B. **83**, 205101 (2011).
[15] A. A. Burkov, and L. Balents, Phys. Rev. Lett. **107**, 127205 (2011).
[16] G. B. Halász, and L. Balents, arXiv:1109.6137v1(2011).
[17] G. Xu, *et al.* Phys. Rev. Lett. **107**, 186806 (2011).
[18] D. Xiao, J. Shi, and Q. Niu, Phys. Rev. Lett. 95, 137204 (2005).
[19] H. B. Nielsen and M. Ninomiya, Nuclear Physics B **185**, 20 (1981).
[20] A. Rycerz, J. Tworzydlo & C. W. J. Beenakker, Nature Physics **3**, 172-175 (2007).
[21] D. Gunlycke, and C. T. White, Phys. Rev. Lett. **106**, 136806 (2011).
[22] D. Xiao, W. Yao and Q. Niu, Phys. Rev. Lett. **99**, 236809 (2007).
[23] W. Yao, D. Xiao, and Q. Niu, Phys. Rev. B. **77**, 235406 (2007).
[24] D. Xiao, G. Liu, W. Feng, X. Xu, and W. Yao, Phys. Rev. Lett. **108**, 196802 (2012).
[25] T. Cao, G. Wang, W. Han, H. Ye, C. Zhu, J. Shi, Q. Niu, P. Tan, E. Wang, B. Liu, and J. Feng, Nature Communications 3, 887 (2012).
[26] M. A. H. Vozmediano, M. I. Katsnelson, and F. Guinea, Physics Reports **496**, 109 (2010).
[27] F. Guinea, M. I. Katsnelson, and A. K. Geim, Nature Physics **6**, 30 (2009).
[28] N. Levy, S. A. Burke, K. L. Meaker, M. Panlasigui, A. Zettl, F. Guinea, A. H. C. Neto, and M. F. Crommie, Science **329**, 544 (2010).
[29] N. Nagaosa, *et al.* Rev. Mod. Phys. **82**, 1539 (2010).
[30] Y. Ran, Y. Zhang, and A. Vishwanath, Nature Physics 5, **298** (2009).